

Geo-Electrical Resistivity Investigation of Mineral Bearing Rocks in Rongo Gold Mining Area in Migori County

¹Dennis Ombati, ¹Ambusso Willis, ²Githiri John and ³Erick Nyakundi

¹*Department of Physics, Kenyatta University.*

²*Department of Physics, Jomo Kenyatta University of Agriculture and Technology.*

³*Department of physics, Kisii University.*

Abstract: *Rongo Gold field forms part of the Lake Victoria greenstone belt and is a highly prospective area. However, it has to date been underexplored due to overburden which obscure the mineralized zones beneath. An electrical resistivity survey was used to detect gold bearing rocks and dense bodies of rocks within host formation in Kamwango area of Rongo district, Migori County. To achieve this, a terrameter (ABEM SAS 1000) was used to determine apparent resistivities using Wenner and Schlumberger configurations. For good vertical resolution, Wenner array was employed to map horizontal structures where a total of 30 stations were done with a probe depth of 45m. Values from Wenner array were used to plot a contour map using Surfer 10 software. The eastern central part of the study area (40km²) is a region of low resistivity as seen from the contour map. Sounding was done on this region of low resistivity along transects using Schlumberger array where a total of 8 stations were sounded as identified from the contour map. IP2WIN software was used to process and model the apparent resistivity values to get true resistivity values. Soundings done on this region gave an average basement depth of 21.86m and a steady rise depth of 32.68m which indicate the depth at which the country rock was hit. High resistivity values indicate the compact volcanic Nyanzian system rocks that are porphyritic, andesites and dacites. The values go up to 1000 Ω m in some parts of the study and the depth is in the range between 40m and 130m. Depths with low resistivity are composed of the highly fractured volcanics with resistivity as low as 13 Ω m. The subsurface and the weathered section also have low values due to presence of groundwater. The conductive zones give resistivity values that correspond to mineral ores that bear gold and related minerals.*

Key words: *Mineralized zones, greenstone belt, electrical resistivity, conductive zones, Kamwango.*

Date of Submission: 02-08-2020

Date of Acceptance: 17-08-2020

I. Introduction

Kamwango area of Rongo is 380 km west of the city of Nairobi in Kenya. It forms part of the Lake Victoria greenstone belt which is endowed with gold deposits. This area which is 60km to the north of the Tanzanian border covers Archaean age metavolcanics and granites where records of gold production within the Nyanzian system are historically known (Ogola, 1995). The gold mineralization in the area occurs in quartz veins and in massive sulphide impregnations (Shackleton, 1946). Artisanal mining is presently active on the Kamwango area. Gold mining has been done in cross-cutting quartz veins, banded iron formation; strata bound horizons in tuffs and alluvial deposits, with the main mines located at Macalder, Masara and Kehancha (Shackleton, 1946).

II. Geologic setting

The area is covered by volcano-sedimentary sequences and intrusive rocks of the Migori greenstone belt which is part of the Archaean Tanzanian craton. Gold is hosted in quartz veins and is associated with massive sulphides like pyrrhotite, pyrite, chalcopyrite, and galena. (Ralph, 2003).

According to Shackleton (1946), intrusive granites have played an important role in the mineralization of the south Nyanza gold field. The largest of these granites, extending from Lake Victoria to the Isuria escarpment, is in contact with Nyanzian rocks (banded ironstones and concentrations of basic rocks) along the entire length of the gold field's southern boundary, and has mineralized a tract of Nyanzian rocks up to three miles in width known as the Migori gold belt. Mineralization is not confined to anyone particular rock type but certain bands are more susceptible to it, notably shales and banded ironstones.

The figure 1.1 below shows the map indicating the study area which is magnified alongside and bounded by the coordinates 675000-683000 Easting (m) and 9918000-9928000 Northing (m).

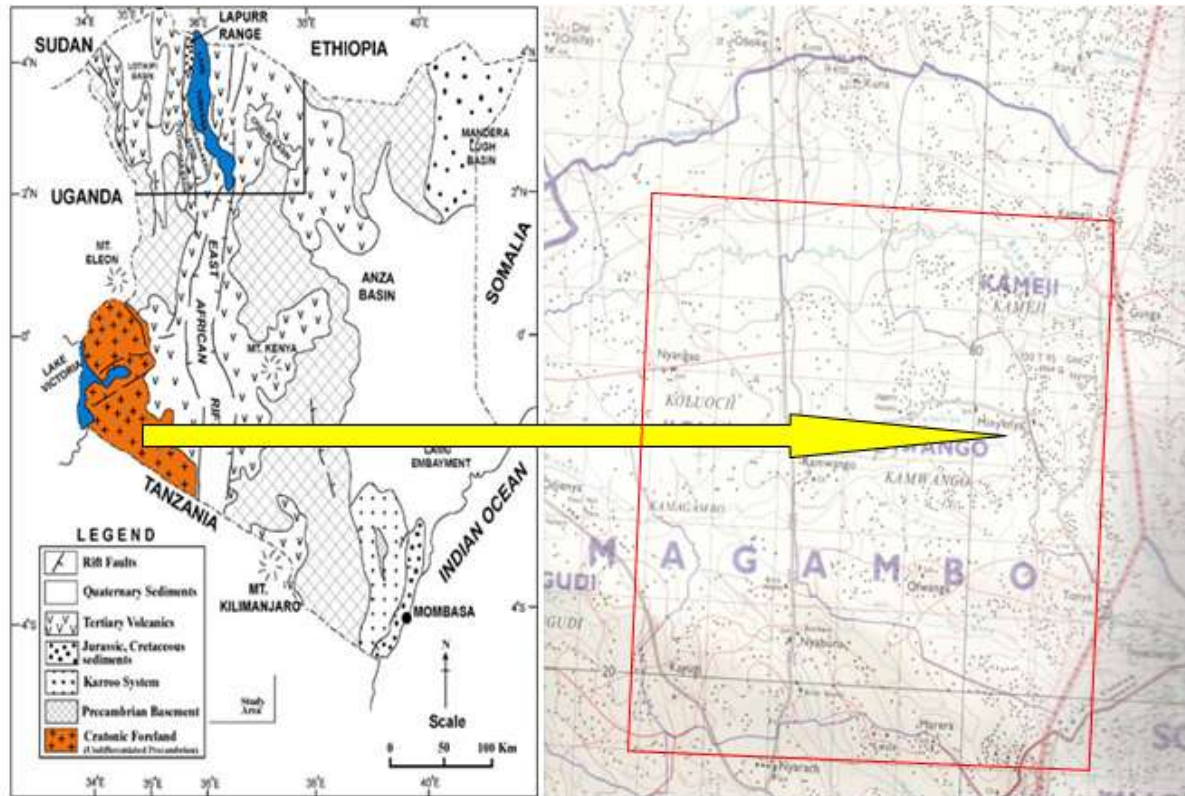


Figure 1.1: Geological map of Kenya locating Kamwango area of Rongo, Migori County. (www.epgeology.com)

III. Methodology

Electrical resistivity is a geophysical method that is utilized in profiling geoelectric structures to locate mineral deposits and aquifers. Hence, as one of the geophysical methods of exploration, electrical prospecting methods have been used for a long time in geological and geotechnical engineering (Keary and Brooks, 1991). The resistivity method has its origin in the 1920's courtesy of the Schlumberger brothers but it still suffices for initial investigations.

General array

The figure 3.1 below shows the general arrangement of the electrodes. The red coloured represent the potential electrodes and the green coloured represent the current electrodes.

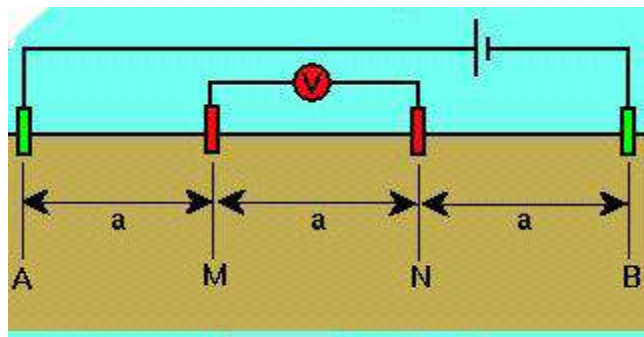


Figure 3.1: General electrode Configuration (Sultan, 2010)

Mathematical Formulation

Resistivity studies in geophysics (Sultan, 2010) begin with:

$$\rho = \frac{2\pi\Delta v}{IG} \tag{3.3}$$

Where G = geometrical factor = $\frac{1}{AM} - \frac{1}{BM} - \frac{1}{AN} + \frac{1}{BN}$ (3.4)

Wenner configuration

Figure 3.2 below shows Wenner configuration. In this configuration, the separation between adjacent electrodes are equal to **a**. the four electrodes; potential electrodes M, N and current electrodes A, B, are collinear

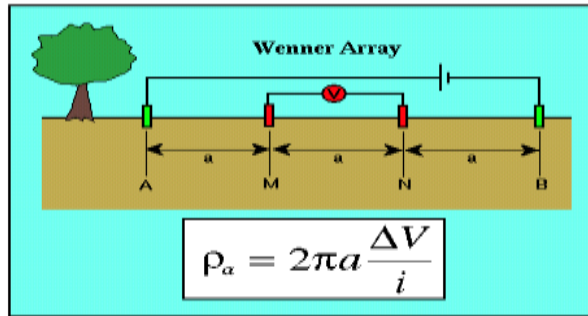


Figure 3.2: Wenner Array and formula for calculating apparent resistivity (Sultan, 2010)

The formula for determining apparent resistivity can be derived as shown in equations 3.5, 3.6, and 3.7 below.

$$\rho_a = \frac{2\pi\Delta v}{I \left[\frac{1}{AM} - \frac{1}{BM} - \frac{1}{AN} + \frac{1}{BN} \right]} \tag{3.5}$$

$$\rho_a = \frac{2\pi\Delta v}{I \left[\frac{1}{a} - \frac{1}{2a} - \frac{1}{2a} + \frac{1}{a} \right]} \tag{3.6}$$

$$= \frac{2\pi a \Delta v}{I} \tag{3.7}$$

Schlumberger configuration

In Schlumberger configuration, The M, N electrodes are between A, B and they are placed symmetrically at the center. The inter-electrode spacing is not constant as shown in figure 3.3 below

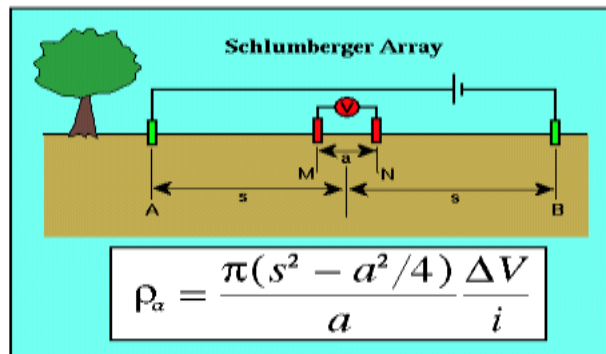


Figure 3.3: Schlumberger Array and formula for calculating apparent resistivity (Sultan, 2010)

Using the total potential at a point on the array equation (Parasnis, 1997)

$$V = \frac{I\rho}{2\pi} \left(\frac{1}{r} - \frac{1}{r'} \right) \tag{3.8}$$

$$V = \frac{I\rho}{2\pi} \left(\frac{1}{L+x} - \frac{1}{L-x} \right) \tag{3.9}$$

$$\frac{dV}{dx} = -\frac{I\rho}{2\pi} \left[\frac{1}{(L+x)^2} - \frac{1}{(L-x)^2} \right] = -\frac{I\rho}{\pi L^2} \tag{3.10}$$

$$= -\frac{\pi L^2}{I} \tag{3.11}$$

$$= -\frac{\pi L^2 \Delta v}{2I} \tag{3.12}$$

Where $\frac{\pi L^2}{2I}$ is the constant of configuration / array constant.

Deduction of the variation of resistivity with depth beneath a given point on the ground is the object of VES. This resistivity is then correlated with the geological information available in order to make an inference of the resistivities of the layers present with depths.

IV. Data Analysis and Discussion of Results

In this study, A GPS (global positioning system) was used in locating the various stations. A total of 30 (thirty) stations were done using the wenner configuration (appendix II) as indicated using the blue asterix, 8(eight) stations were done using configuration as indicated using the green small triangles of figure 4.1.

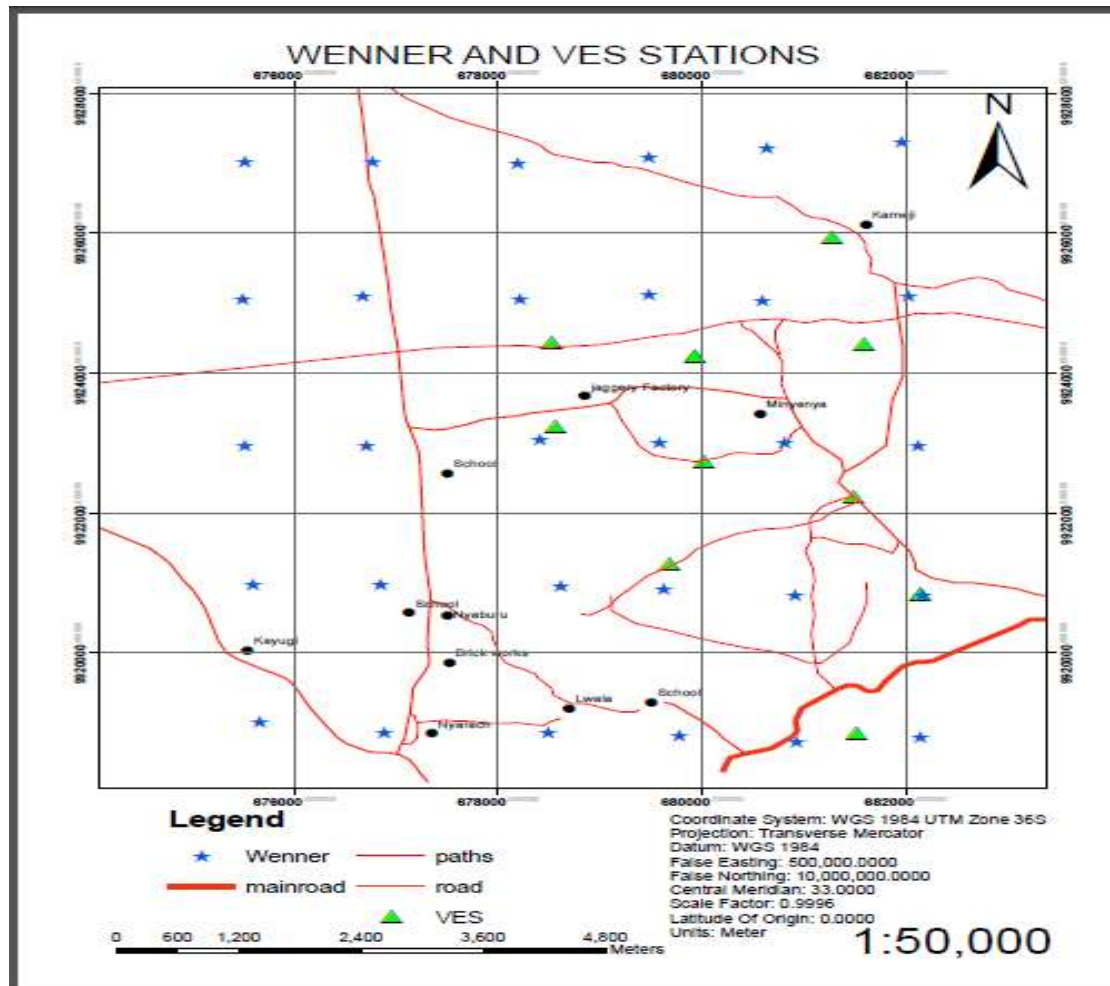


Figure 4.1: Shows profiles (blue marks) and VES transects (green marks)
(Courtesy of ARCGIS software)

Curve Matching

Curve matching is a substantially accurate and dependable method of interpretation in electric sounding and involves the comparison of field profiles with characteristic curves. Then on-linear inverse problems are solved using the standard linearized inversion approach based on iterative processes. Inversion processes update the model parameter at each step to best fit the observed data by using damped least-squares equation 4.1 (Menke, 1984).

$$\Delta m = (G^T G + \beta^2 I)^{-1} G^T \Delta d \tag{4.1}$$

where Δm is the parameter correction vector, Δd is the data difference vector, G is the Jacobian matrix containing partial derivatives of data with respect to the initial model parameter, I is the identity matrix, and the term β is called the damping factor which is a scalar quantity that controls both the speed of convergence and solution.

The conversion of the apparent resistivity which is a function of electrode spacing to the true resistivity being as a function of depth is achieved by the Ip2win software using the equation (4.2). (Reynolds, 1998)

Where,

$$\rho_a(s) = s^2 \int_0^\infty T(\lambda) J_1(\lambda s) \lambda d\lambda \tag{4.2}$$

- S is half of the current electrode spacing (AB/2)
- $T(\lambda)$ is the resistivity transform function
- J_1 denotes the first order Bessel function of the first kind
- λ denotes the integral variable

V. Qualitative Interpretation

Contour Map

The data that was collected through the equipment was tabulated and arranged in excel sheets and thereafter conversion of the geographical coordinates from GPS system to UTM. The data was then plotted on Surfer, and a contour map generated as shown in Figure 5.1.

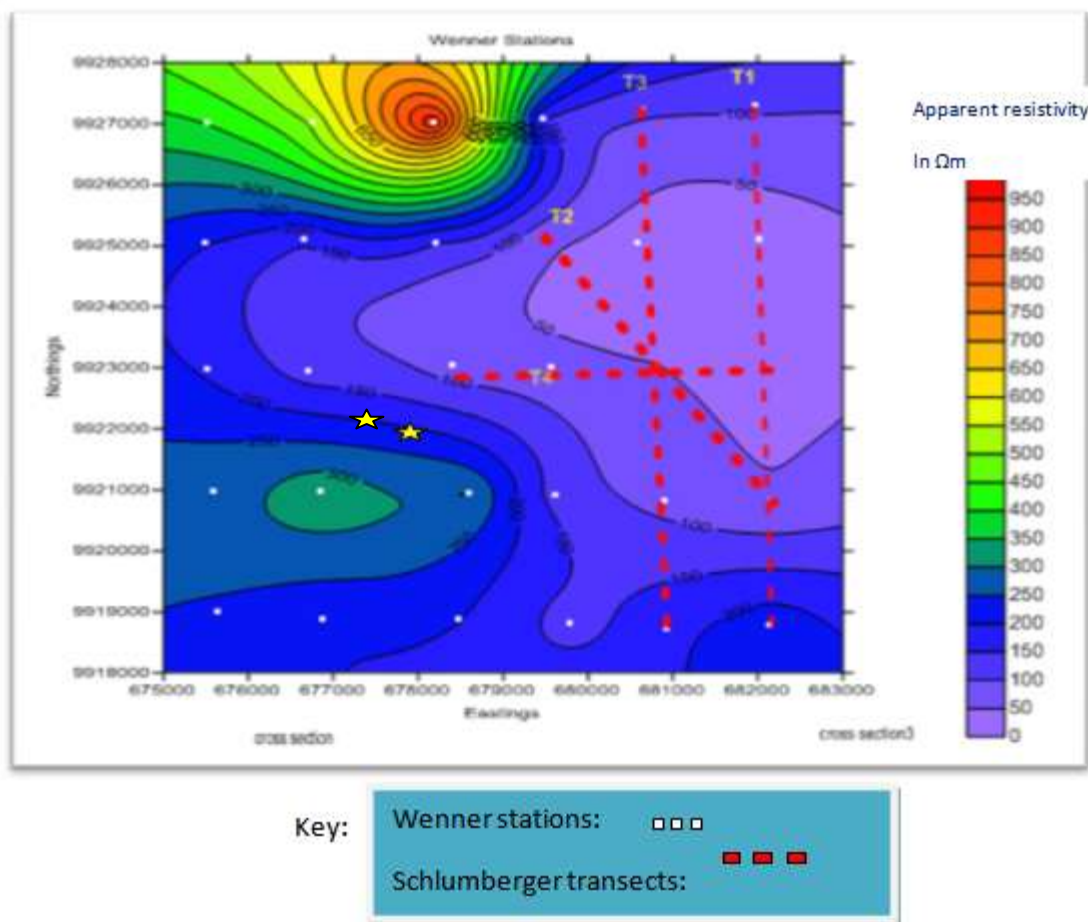


Figure 5.1: A contour map showing profiles for wenner and transects for schlumberger.

The central and Eastern regions have the lowest resistivity values and this indicates a conductive buried ore body as shown in figure 5.1. Metallic and conductive minerals may be disseminated in the said regions. Gold that is conductive occurs at the probe depth of 45m. The northern tip has the greatest resistivity values. The sounding was conducted on the values with the least resistivity values from the profiles within an area of approximately 10 Km². 1 IP2WIN Curve Fitting

The tables alongside the curves in figures 5.4a, 5.4b, 5.4c, 5.4d, 5.4e, 5.4f, and 5.4g give information about resistivity layer. Resistivity value in each ground layer is displayed in ρ column. Alt column is altitude column or depth from VES point elevation. Information of depth from surface is displayed in d column. Information of each layer thickness with different resistivity value is displayed in g column. The black curve is the observed while the red is the calculated. Red and Blue curve give information about the relation between AB/2 and apparent resistivity value. Blue curve give information about resistivity value variation.

This curve fitting achieved an average basement depth of 21.86m at accuracy of 5.635% (good fit with average correlation of 94.365%). This accuracy is less than the maximum accepted 10%. It therefore implies that the curves are accurate enough to be used in deduction of the different layers' depth and resistivities at the sounding station. For VES 1, the curve outlines three layers: the first layer with a resistivity of 49.9 Ω m has a thickness of 1.17m; the second layer with a resistivity of 6.87 Ω m has a thickness of 1.31 m; the third layer with a resistivity of 148 Ω m has a thickness of 28.6m and a basement being hit from depth of 31.1m. The fitting has an accuracy of 7.36% (Figure 5.4 a). For VES 2, the curve outlines three layers: the first layer with a resistivity of 38.2 Ω m has a thickness of 0.451m; the second layer with a resistivity of 2.1 Ω m has a thickness of 0.862 m; the third layer with a resistivity of 32.2 Ω m has a thickness of 15.5m and a basement being hit from a depth of 16.8m. The fitting has an accuracy of 6.8% as in figure 5.4 b.

For VES 3, the curve outlines three layers: the first layer with a resistivity of 72.6 Ωm has a thickness of 48.9mm; the second layer with a resistivity of 19.5Ωm has a thickness of 71.4cm; the third layer with a resistivity of 31.4 Ωm has a thickness of 15.3m and a basement being hit from depth of 16.1m. The fitting has an accuracy of 4.21% as shown by figure 5.4 c. For VES4, the curve outlines three layers: the first layer with a resistivity of 500 Ωm has a thickness of 0.629m; the second layer with a resistivity of 15.8 Ωm has a thickness of 2.85 m; the third layer with a resistivity of 31.8 Ωm has a thickness of 23.7m and a basement being hit from depth of 27.1m. The fitting has an accuracy of 4.83% (Figure 5.4 d).

For VES 5, the curve outlines three layers: the first layer with a resistivity of 505 Ωm has a thickness of 0.627m; the second layer with a resistivity of 16Ωm has a thickness of 2.9 m; the third layer with a resistivity of 31.7Ωm has a thickness of 23.2m and a basement being hit from depth of 26.8m. The fitting has an accuracy of 4.99% (Figure 5.4 e). For VES 6, the curve outlines three layers: the first layer with a resistivity of 148Ωm has a thickness of 1.74m; the second layer with a resistivity of 19.2Ωm has a thickness of 6.54 m; the third layer with a resistivity of 30304 Ωm has a thickness of 12.4m and a basement being hit from depth of 20.7m. The fitting has an accuracy of 6.51% (Figure 5.4 f). For VES 7, the curve outlines three layers: the first layer with a resistivity of 286Ωm has a thickness of 1.81m; the second layer with a resistivity of 2025Ωm has a thickness of 3.13 m; the third layer with a resistivity of 189Ωm has a thickness of 5.21m and a basement being hit from depth of 10.2m. The fitting has an accuracy of 4.42% (Figure 5.4 g). In figure 5.4 h (VES 8) the curve outlines three layers: the first layer with a resistivity of 2632 Ωm has a thickness of 0.566m; the second layer with a resistivity of 243Ωm has a thickness of 5.08 m; the third layer with a resistivity of 22.2 Ωm has a thickness of 14.5m and a basement being hit from depth of 20.1m. The fitting has an accuracy of 5.96%.

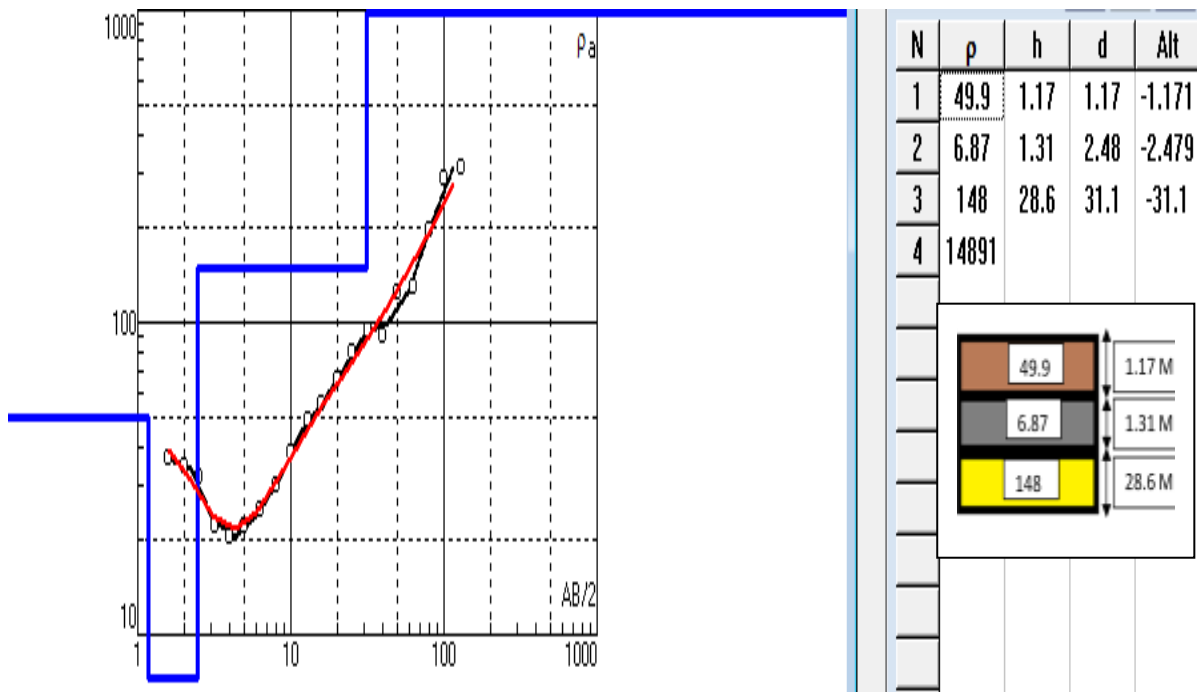


Figure 5.4 a: VES 1 curve matching (RMS=7.36%)

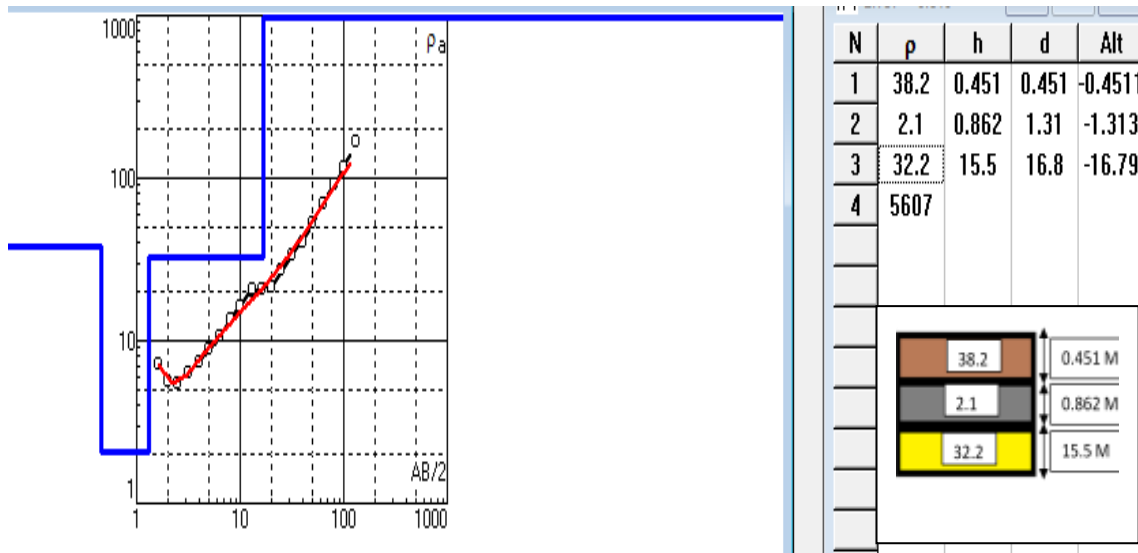


Figure 5.4 b: VES 2 curve matching (RMS=6.8%)

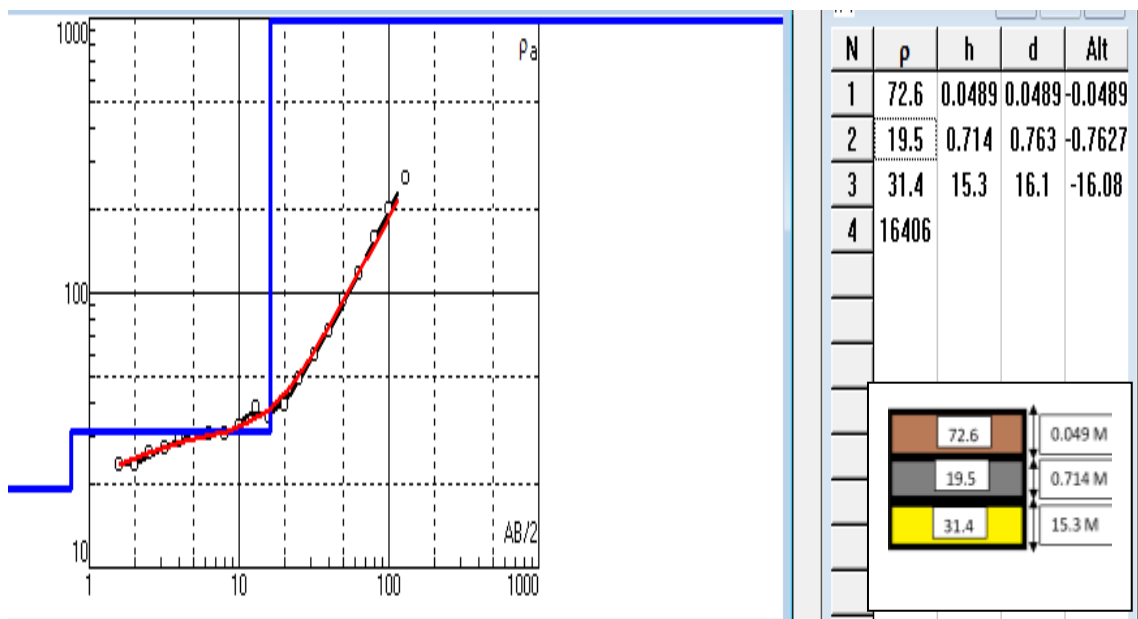


Figure 5.4 c: VES 3 curve matching (RMS=4.21%)

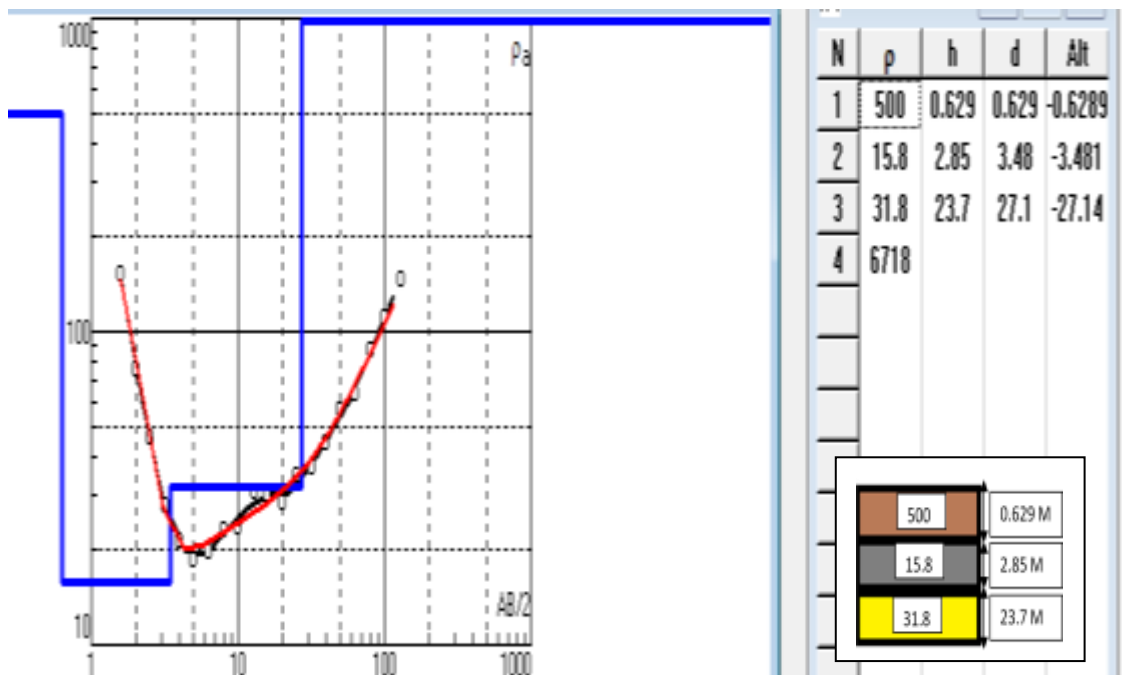


Figure 5.4 d: VES 4 curve matching (RMS=4.83%)

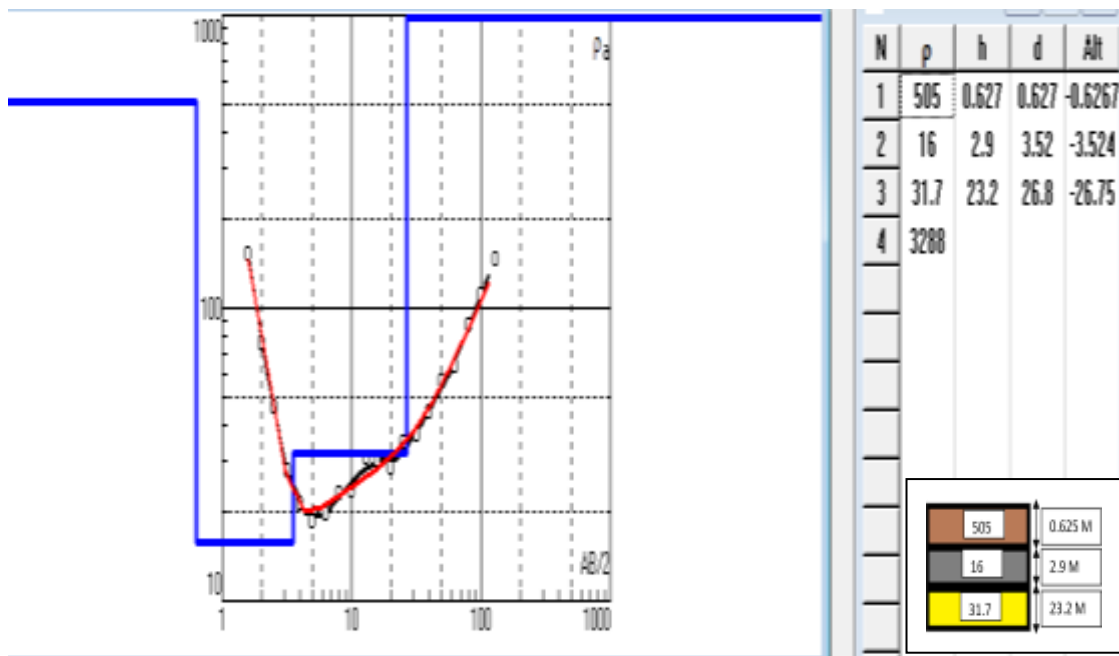


Figure 5.4 e: VES 5 curve matching (RMS=4.99%)

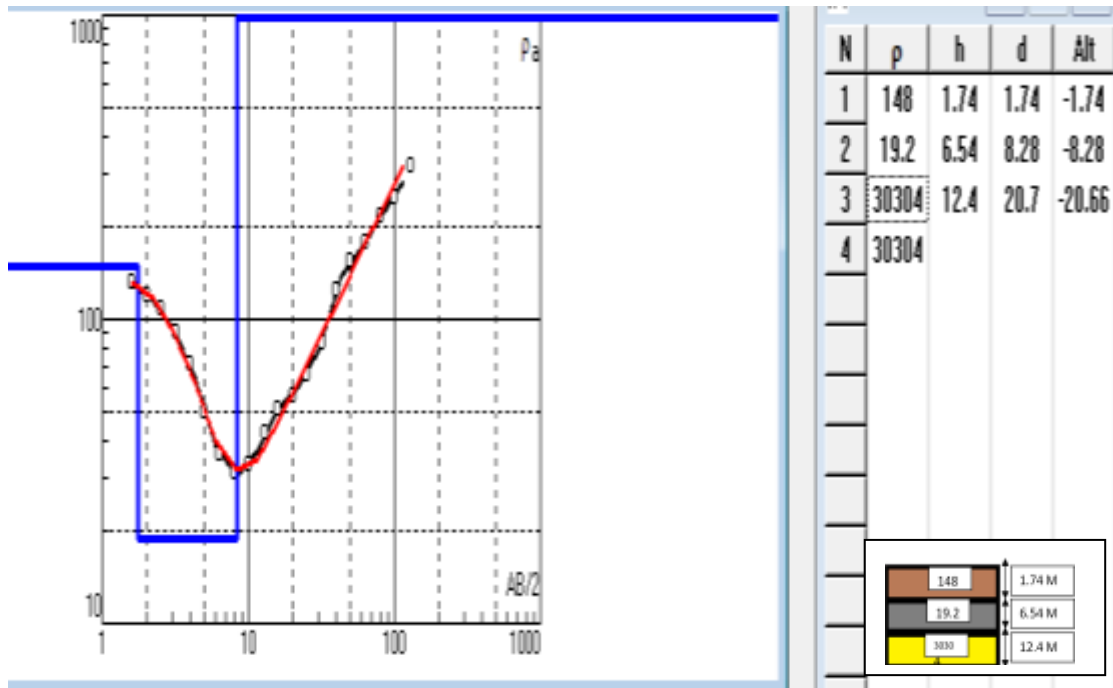


Figure 5.4 f: VES6 curve matching (RMS=6.51%)

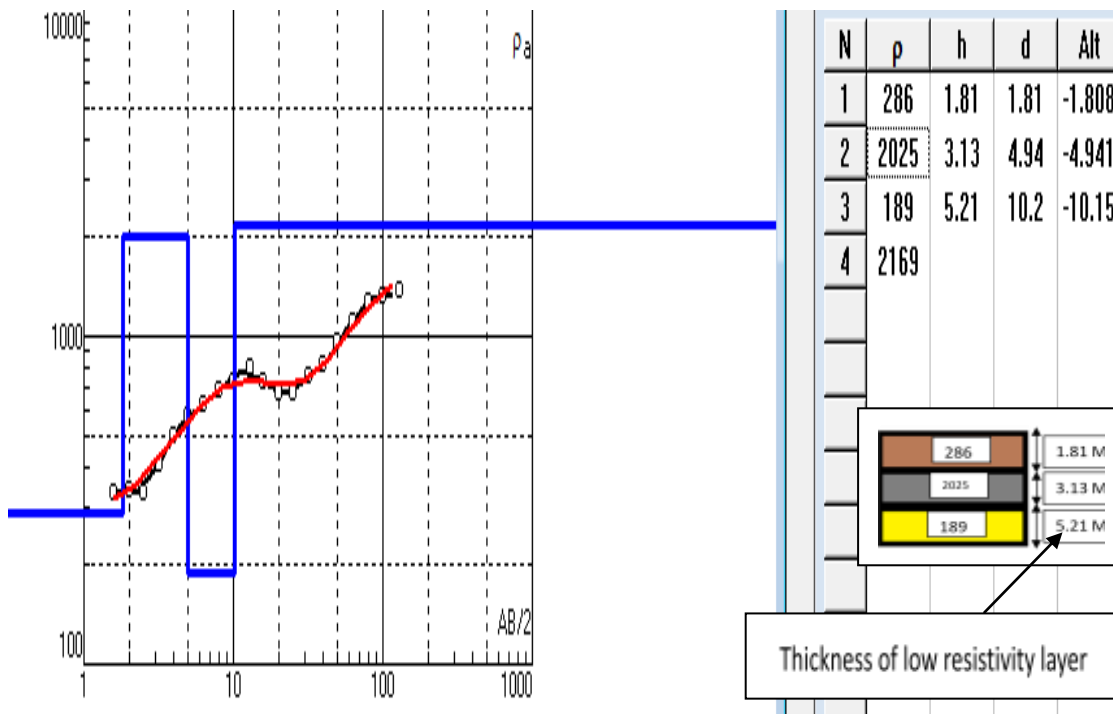


Figure 5.4 g: VES7 curve matching (RMS=4.42%)

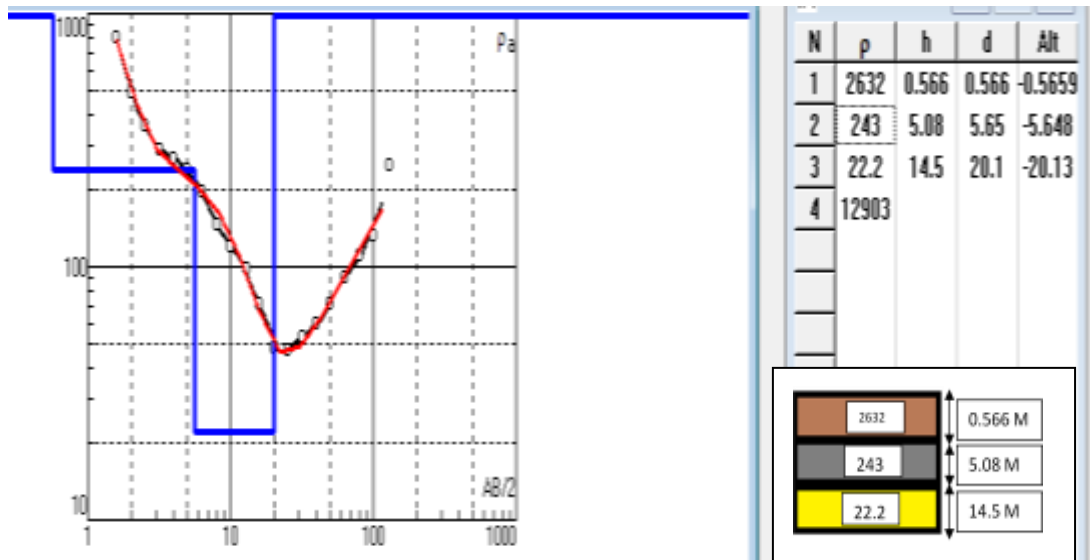


Figure 5.4 h: VES8 curve matching (RMS=5.96%)

Table 5.1: Summary of layer thickness with corresponding resistivity for the VES stations

VES	LAYER 1		LAYER 2		LAYER 3		LAYER 4		ERROR
	No.	ρ (Ω m)	h (m)	ρ (Ω m)	h (m)	ρ (Ω m)	h (m)	ρ (Ω m)	
1	49.9	1.17	6.87	1.31	148	28.6	14891	∞	7.36
2	38.2	0.451	2.1	0.862	32.2	15.5	5607	∞	6.80
3	72.6	0.0489	19.5	0.714	31.4	15.3	16406	∞	4.21
4	500	0.629	15.8	2.85	31.8	23.7	6718	∞	4.83
5	505	0.627	16	2.9	31.7	23.2	3288	∞	4.99
6	148	1.74	19.2	6.54	30304	12.4	30304	∞	6.51
7	286	1.81	2025	3.13	189	5.21	2169	∞	4.42
8	2632	0.566	243	5.08	22.2	14.5	12903	∞	5.96

Pseudo cross-sections models

The pseudo section is useful as a means to present the measured apparent resistivity values in a pictorial form, and as an initial guide for further quantitative interpretation. Red colouration is representative of litho-layers with high resistivity values while those with blue are designated to those of less resistivity values. Different colours by the model are assigned to geological layers that have similarities in geo-electric properties. Red colour (near the surface) corresponds to regions of less electrical conductivity (figures 5.5 a, 5.5 d, and 5.5 f). This could be an implication of holes left by artisanal miners or outcrops of the granites and volcanics of the Nyanzian system. The rocks are intruded by granites and dolerites and in other places are overlain by tertiary volcanics (Ogola, 1995).

Blue colours are indicative of metallic minerals that are conductive. The region between VES 1 and VES 3 there is a near surface formation of very low resistivity to a depth of about 14m and directly below VES 2. This is a highly conductive material that can be an auriferous structure or a sulphide impregnation that hosts gold and related minerals. The region of low resistivity has a big spread between VES 1 and VES 6 especially the area bounded by the yellow colouration in the figure 5.5 and figure 5.5 (a) below. The highest resistivity in this area is about 70 Ω m. This is still low and it matches with most mineral ores gold inclusive. The region between VES 7 and VES 8 is a region of high resistivity which is about 500 Ω m (figure 5.5 c). This is indicative of a volcanic or granitic intrusion which could be slightly weathered. The region however is a narrow strip that

may not be easily detected following the principle of suppression. This is particularly a problem when three or more layers are present and their resistivities are ascending or descending with depth. The middle intermediate layer may not be evident on the field curve.

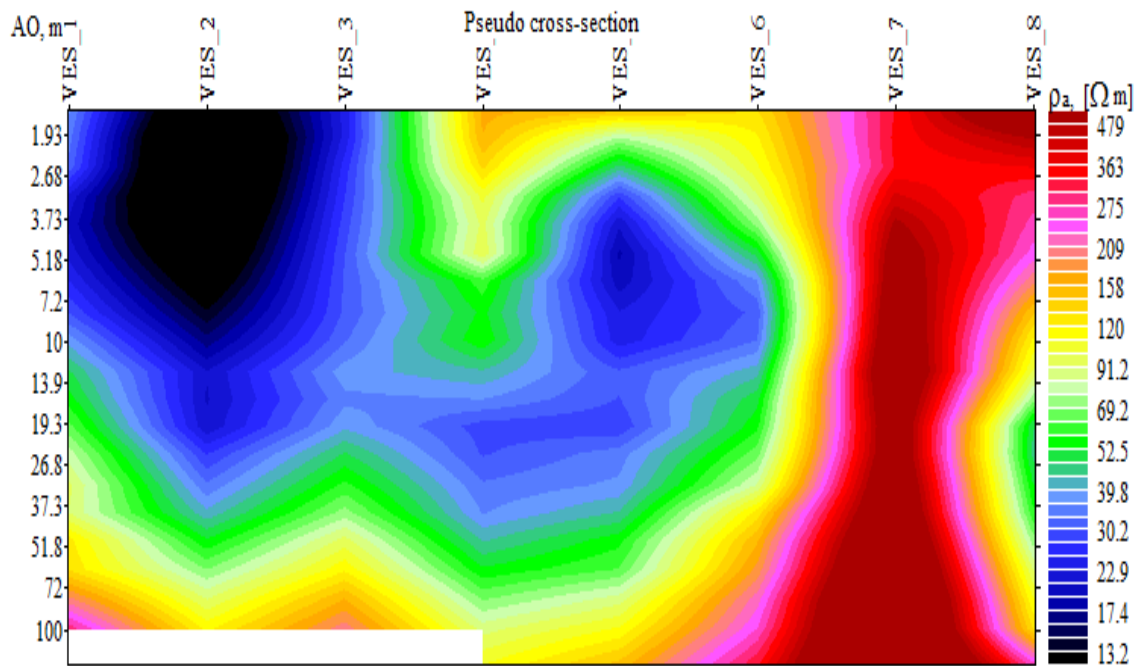


Figure 5.5: Pseudo cross-section showing spatial layer distribution for all VES 1-8

Table 5-2 below shows the summary of the layer lithology of the study area and the implied formations

Table 5.2: Layer Lithology

DEPTH (in meters)	RESISTIVITY (Ohm)	FORMATION
0-1.7	120-90	Soil formation
1.7 – 7.00	13.85	Moist sub-base
7.70 – 10.5	50-70	Weathered volcanics
10.5 – 40.30	16.2-50	Highly Fractured volcanic (water bearing)
40.30– 120	70-100	Compact formation of the volcanics



Table 5.3: Layer Lithology of bore hole for VES 2 about 4 km from the study area

Depth (m)	Resistivity (Ohmm)	Interpretation
0.0 – 2.5	1364.0	Sandy top soils
2.5 – 9.8	70.0	Weathered Pyroclastics & sediments
9.8 – 80.0	420.0	Fresh Pyroclastics & sediments
80 - 190	288.0	Highly weathered pyroclastics and gravels (aquiferous)
Below 190.0	520.0	Weathered to fresh rock

A borehole is recommended to be drilled at the site of VES- 2 to a maximum depth of about 200 m bgl. This will ensure that the deeper aquifer will be fully penetrated.

Table 5.4: Kamwango drill results (adopted from www.stockportexploration.com)

KG-11-02
Elevation 4548 feet;
-0.69883, 34.59661

KAMWANGO DRILL RESULTS

2012 Drill Results			2003-04 Drill Results		
Drill hole	Gold (g/t)	Width (m)	Drill hole	Gold (g/t)	Width (m)
KG-11-01	3.34	5.96	DDH-1	34.5	2.96
Including	4.55	4.15	DDH-3	1.4	20.0
KG-11-02	10.68	4.8	Including	2.13	5.5
Including	51.6	0.81	DDH-4	81.4	2.55
KG-11-02	0.94	3.4	DDH-6	0.4	11.7
KG-11-03	4.14	3.83	DDH-7	2.8	7.6
Including	5.0	3.13	Including	3.95	5.3
KG-11-03	2.8	4.38			
Including	4.16	2.77			

Shallow drilling: All current intercepts run between 25 m – 60 m vertical depth.

VI. Conclusions and Recommendations

Conclusion

Mapping out of auriferous units and a better comprehension of ore characteristics in Kamwango area, using profiling and sounding, has been made simple. Ore characteristics include; the thickness, depth to bedrock and fractured/faulted zones which are required for locating points with high potentials for ore body occurrence. From the contour map the central eastern part of the study area at a probe depth of 45m covering an approximate area of 10 Km² indicated low resistivity anomaly. On this region eight soundings were done from which VES1 to VES 6 can be postulated to be having an ore body at shallow depths between 10m to about 70m and covering an approximate area of 6 Km². VES 7 indicates a granitic intrusion of resistivity of about 500Ωm. Soundings done on this region gave an average basement depth of 21.86m and a steady rise depth of 32.68m, which indicate the depth at which the country rock is hit.

From the pseudo cross-sections, auriferous structures, having an east-west trend like all geological structures in the Archaean of the Tanzania craton, have been delineated in deeply weathered volcanic rocks. Related studies in the area are in agreement with this study. Banded iron formations by Mukasa (2001) and pyrrhotite by Oketch (2012) are all hosts for Gold. The drills done by exploration companies such as Stockport, Table 5.5, and African Queens give results that very well match with the findings of this study. Shallow formations that indicate an economically viable deposit have been intercepted. The low resistivity anomaly generally exhibits an East-West to North West-South East range of trend similar to all structures in the Archaean of the Tanzanian craton.

The association of gold with metallic sulphides and oxides which are excellent electrical conductors made it possible to target such ores using geoelectric exploration.

Recommendations

Because any exploration geophysics requires complementary geophysical surveys integrated with geochemical, environmental geophysics and geologic insight, the resistivity survey carried out in Kamwango area cannot be regarded as an end but as a valuable piece of work for further research and development. This study probed a maximum depth of 130m. However, drilling is recommended at VES 1,2,3,5 and 6 to depths of about 60m which have resistivity range between 2 Ωm to about 50 Ωm. There is need to probe greater depths because some mines in the world are as deep as 4km. Therefore, it is recommend Magnetotelluric method to be

employed. Major advantages of Magnetotelluric (MT) method is its unique Capability for exploration to very great depths (hundreds of kilometers) as well as in shallow investigations without using of an artificial power source.

In addition, it is recommended that the geological information of the Kamwango area be updated since the available information is pre-colonial that concentrates on the lower part of Migori greenstone belt leaving out the upper part, Kamwango inclusive. Finally drilling will assist in confirming the presence and exact location in depth of the main ore body which might have potential economic value.

Acknowledgements

I take this solemn opportunity to thank our Almighty God for His rich grace to have guided me in this study thus far. I register my appreciation to Dr. Ambusso Willis for his keen and focused guidance in the development of this work, my second supervisor, Dr. John Githiri, for his attitude and devotion in this study.

References

- [1]. ABEM instruction manual (2010). Terrameter SAS 4000/SAS 1000. Retrieved from <http://www.abem.se/files/upload/manual-terrameter.pdf>.
- [2]. Keary, P and Brooks, M. (1991). An Introduction to Geophysical Exploration, 2nd Edition, Blackwell Scientific Publications, London, 254. Minerals of Kenya. Geological survey bulletin
- [3]. Menke, W. (1984). Geophysical data Analysis, Discrete inverse theory, Academic press Inc. New York.
- [4]. Mukasa, J.K (2001). Magnetic survey of banded iron formation in Migori segment of Nyanza greenstone belt. Master's thesis. Kenyatta University.
- [5]. Ogola, J. S., (1995). Geology and mineral resources of Nyanza province, Western Kenya. Geol. Soc. Afr. 95, pp. 407 - 430.
- [6]. Oketch, F.O. (2012). Exploration of pyrrhotite mineral and its distribution in Kamwango area. Geology project. Nairobi University
- [7]. Parasnis D. S. (1997). Principles of Applied Geophysics, 5th Edition, Chapman and Hall, London, England, 104-176.
- [8]. Ralph. (2003). The Geology of coarse gold formation. Retrieved from <http://www.nuggetshooter.com/articles/CRGeologyofcoarsegoldformation.html>
- [9]. Reynolds, J. M. (1998). An Introduction to Applied and Environmental Geophysics. Wiley.
- [10]. Shackleton, R.M. (1946). Geology of the Migori Gold belt and adjoining areas. Rep. geol. surv. kenya, 10.
- [11]. Sultan, A.S. (2010). Geophysical exploration for gold and associated minerals, case study: Wadi El Beida area, South Eastern Desert, Egypt.

Dennis Ombati, et. al. "Geo-Electrical Resistivity Investigation of Mineral Bearing Rocks in Rongo Gold Mining Area in Migori County." *IOSR Journal of Applied Geology and Geophysics (IOSR-JAGG)*, 8(4), (2020): pp 28-40.